



Validation of ATR FT-IR to identify polymers of plastic marine debris, including those ingested by marine organisms

Melissa R. Jung^a, F. David Horgen^a, Sara V. Orski^b, Viviana Rodriguez C.^b, Kathryn L. Beers^b, George H. Balazs^c, T. Todd Jones^c, Thierry M. Work^d, Kayla C. Brignac^e, Sarah-Jeanne Royer^f, K. David Hyrenbach^a, Brenda A. Jensen^a, Jennifer M. Lynch^{g,*}

^a College of Natural and Computational Sciences, Hawai'i Pacific University, Kaneohe, HI, United States

^b Materials Science and Engineering Division, National Institute of Standards and Technology, Gaithersburg, MD 20899, United States

^c Pacific Islands Fisheries Science Center, National Marine Fisheries Service, Honolulu, HI, United States

^d U.S. Geological Survey, National Wildlife Health Center, Honolulu Field Station, Honolulu, HI, United States

^e School of Ocean, Earth Science, and Technology, University of Hawai'i at Manoa, Honolulu, HI, United States

^f Daniel K. Inouye Center for Microbial Oceanography: Research and Education, University of Hawai'i at Manoa, Honolulu, HI, United States

^g Chemical Sciences Division, National Institute of Standards and Technology, Kaneohe, HI, United States

ARTICLE INFO

Keywords:

Sea turtles
Pacific Ocean
Marine plastic debris
Plastic ingestion
Fourier transform infrared spectroscopy
Polymer identification

ABSTRACT

Polymer identification of plastic marine debris can help identify its sources, degradation, and fate. We optimized and validated a fast, simple, and accessible technique, attenuated total reflectance Fourier transform infrared spectroscopy (ATR FT-IR), to identify polymers contained in plastic ingested by sea turtles. Spectra of consumer good items with known resin identification codes #1–6 and several #7 plastics were compared to standard and raw manufactured polymers. High temperature size exclusion chromatography measurements confirmed ATR FT-IR could differentiate these polymers. High-density (HDPE) and low-density polyethylene (LDPE) discrimination is challenging but a clear step-by-step guide is provided that identified 78% of ingested PE samples. The optimal cleaning methods consisted of wiping ingested pieces with water or cutting. Of 828 ingested plastics pieces from 50 Pacific sea turtles, 96% were identified by ATR FT-IR as HDPE, LDPE, unknown PE, polypropylene (PP), PE and PP mixtures, polystyrene, polyvinyl chloride, and nylon.

1. Introduction

Plastic is one of the most persistent and abundant types of marine debris (Rios et al., 2007). For instance, high concentrations of up to 334,271 pieces/km² have been estimated floating in the North Pacific central gyre, where this material is concentrated by wind-driven ocean currents (Moore et al., 2001; Howell et al., 2012). The production of plastic and associated marine plastic debris continues to rise (Geyer et al., 2017; Jambeck et al., 2015; Bakir et al., 2014; Hoarau et al., 2014), with an estimated 4.8 million metric tons to 12.7 million metric tons of plastic debris entering the marine environment each year (Jambeck et al., 2015). As marine plastic debris continues to accumulate, long-term environmental, economic, and waste management problems grow, including significant economic costs for prevention and clean-up (Singh and Sharma, 2008; McIlgorm et al., 2011). Increasing awareness of the possible ecological impacts of marine debris has stimulated research to quantify and understand the incidence and

magnitude of plastic ingestion by marine animals (Andrady, 2011; Provencher et al., 2017).

Ingestion of plastic debris has been documented in marine species across a range of sizes and biological complexity: from microscopic zooplankton to large vertebrates (Hoss and Settle, 1990; Nelms et al., 2015; Cole and Galloway, 2015; Unger et al., 2016). The size of ingested plastic debris occupies a large range, evidenced by filter feeders, like oyster larvae, which can ingest microplastics as small as 0.16 µm diameter (Cole and Galloway, 2015), while large items such as part of a car engine cover (650 mm × 235 mm) have been found in the gastrointestinal tracts of sperm whales (*Physeter macrocephalus*) (Unger et al., 2016). Sea turtles are a good indicator of plastic debris occurrence in the natural environment as studies have documented ingestion around the world including coastal Florida, southern Brazil, the Central Pacific, and Mediterranean Sea (Bjorndal et al., 1994; Bugoni et al., 2001; Clukey et al., 2017; Tomás et al., 2002). Sea turtles ingest a variety of plastic items of varying types, sizes, and morphologies, including pieces

* Corresponding author at: Chemical Sciences Division, National Institute of Standards and Technology, 45-045 Kamehameha Hwy, Kaneohe, HI, United States.
E-mail address: jennifer.lynch@nist.gov (J.M. Lynch).

of bags, rope, fishing line, foam, and fragments of less flexible plastic that range in size from microplastics (< 5 mm on largest edge) to macroplastics (> 25 mm) with fragments up to 10 cm observed (Bugoni et al., 2001; Tomás et al., 2002; Clukey et al., 2017). A study by Clukey et al. (2017) showed that a total of 2880 plastic debris items were ingested by 37 olive ridley (*Lepidochelys olivacea*), nine green (*Chelonia mydas*), and four loggerhead (*Caretta caretta*) pelagic sea turtles that were incidentally taken by longline fisheries in the North Pacific Ocean. Plastic fragments constituted 79.5% of the total debris while 12.5% were thin plastic sheets (e.g., bags and thin packaging material) and 6.1% were line or rope (Clukey et al., 2017). While the commercial use of some ingested plastics, such as bags and fishing line, can be easily identified by visual inspection, few pieces are found completely intact and their original origin is difficult to discern (Hoss and Settle, 1990). Fortunately, plastic manufacturers and standards organizations have developed a standard identification system for general classes of plastic that can be used to help identify their likely intended commercial use.

Most plastic consumer goods are labeled with standardized resin codes marked inside a triangle (ASTM, 2013), signifying the chemical composition of the main polymer, which is used to sort and recycle compatible materials. These include polyethylene terephthalate (PETE, #1), high-density polyethylene (HDPE, #2), polyvinyl chloride (PVC, #3), low-density polyethylene (LDPE, #4, which also currently includes linear LDPE [LLDPE]), polypropylene (PP, #5), polystyrene (PS, #6), and other polymers (#7). These codes are rarely present or legible in recovered plastic debris or small plastic fragments, hence identification of the polymer must be accomplished using chemical testing. Characterizing unknown polymers helps illuminate many of the issues surrounding marine debris. Knowing the polymer structure will aid in determining the transport and fate of debris pieces in the environment, such as the effect of material density on stratification within the water column or the susceptibility of specific chemical bonds to break under environmental conditions. In addition, different polymers have different affinities for adsorbing chemical pollutants from seawater, suggesting some polymers may present a larger risk of transferring pollutants to marine organisms who ingest them (Rochman et al., 2013; Fries and Zarfl, 2012; Endo et al., 2005; Koelmans et al., 2013). Knowing the predominant polymers found in various habitats or ingested by marine organisms can help focus conservation efforts, including changes to recycling strategies, targeted waste management, or novel approaches in polymer production (Ryan et al., 2009). Furthermore, since certain polymers are more commonly recycled than others (e.g., #2 HDPE compared to #4 LDPE), it is important to be able to distinguish these to monitor the success of waste management techniques.

Several analytical tools have been used to identify the composition of plastic debris (Andrady, 2017). For example, environmental samples from German rivers were analyzed using thermogravimetric analysis connected to solid-phase adsorbents that were subsequently analyzed by thermal desorption gas chromatography mass spectrometry (GC/MS; Dümichen et al., 2015). Fischer and Scholz-Böttcher (2017) used pyrolysis-GC/MS to identify microplastics ingested by North Sea fish. In addition, GC/MS has been utilized to identify indicator chemicals characteristic of different polymers of plastics ingested by Laysan albatross (*Phoebastria immutabilis*) (Nilsen et al., 2014). These methods are limited to only volatile or ionizable compounds, such as small oligomeric fragments or additives within the bulk material. Methods that can analyze the entire sample, and often require less sample preparation, are vibrational spectroscopy measurements such as Raman microspectroscopy (Frère et al., 2016) and Fourier transform infrared (FT-IR) spectroscopy. FT-IR is becoming the most common technique for marine debris polymer identification. It has been used to identify microplastics near the surface of the Ross Sea, from the English Channel, and ingested by zooplankton (Cincinelli et al., 2017; Cole et al., 2014). Recently, Mecozzi et al. (2016) used FT-IR coupled with the Independent Component Analysis (ICA) database and Mahalanobis

Distance (MD) to identify marine plastics ingested by four loggerhead sea turtles in the Mediterranean Sea.

FT-IR spectroscopy offers a simple, efficient, and non-destructive method for identifying and distinguishing most plastic polymers, based on well-known infrared absorption bands representing distinct chemical functionalities present in the material (Verleye et al., 2001; Coates, 2000; Asensio et al., 2009; Beltran and Marcilla, 1997; Noda et al., 2007; Nishikida and Coates, 2003; Ilharco and Brito de Barros, 2000; Guidelli et al., 2011; Rotter and Ishida, 1992; Asefnejad et al., 2011). Structural isomeric polymers, such as HDPE and LDPE, are difficult, yet important, to differentiate. Asensio et al. (2009) and Nishikida and Coates (2003) reported that LDPE had a unique characteristic (yet quite small) band at 1377 cm^{-1} , representing a CH_3 bending deformation, suggesting that even these similar polymers can be distinguished using FT-IR spectra. This band is reportedly absent in HDPE. These polymers differ by the extent of branching with HDPE being a linear PE chain with minimal branching, LLDPE having short alkyl branches off a linear backbone, and LDPE having long PE branches that represent a significant portion of the total chain length. Increased branching will reduce material density, with HDPE densities ranging from 0.94 g/mL to 0.97 g/mL and LLDPE and LDPE densities ranging from 0.90 g/mL to 0.94 g/mL (Peacock, 2000; Verleye et al., 2001). However, chemical weathering, natural aging, and biochemical processes affecting ingested plastics can modify their spectral features, making identification difficult (Mecozzi et al., 2016), which was evident in Brandon et al. (2016) in which 30% of marine debris polyethylene (PE) samples could not be differentiated. These particularly challenging pieces produce confusing spectra due to the similar intensities of bands at 1377 cm^{-1} and 1368 cm^{-1} . No study has yet tested or provided criteria on how to differentiate these.

The goal of this study was to thoroughly assess the validity of attenuated total reflectance (ATR) FT-IR for identifying polymer composition of ingested plastic marine debris. This chemical technique is certainly not new and is common, but our study provides novel details that can help future studies avoid pitfalls, reduce confusion, and increase identification accuracy. We provide a clear guide with strict criteria to differentiate spectra from HDPE and LDPE. Furthermore, we identified and described the most effective cleaning method for preparing ingested plastic samples of three common polymers from pelagic, long-line caught olive ridley sea turtles to obtain high quality spectra. Sample handling was minimized to retain the original sample in a specimen bank for future additional chemical testing. To accomplish these goals, we developed an in-house spectral library from plastic consumer goods marked with resin codes. We validated our library with polymers originating from National Institute of Standards and Technology (NIST) Standard Reference Materials (SRMs)®, polymer standards obtained from scientific vendors, raw polymers sourced from manufacturers, and an additional set of consumer goods with polymer identity unknown to the analyst. PE materials of known density were used to confirm that ATR FT-IR is capable of discriminating between HDPE and LDPE, and to determine if a float/sink test in various dilutions of ethanol could further assist in differentiating these polymers. Using these optimized ATR FT-IR methods, we analyzed 828 ingested plastic items for polymer identity. A subset of these ingested samples was analyzed at NIST using high temperature size exclusion chromatography (HT-SEC) to confirm the accuracy of polymer identification by ATR FT-IR.

2. Methods

2.1. Plastic standards

Plastic standards were obtained from four sources with different degrees of purity or certainty (see Supplemental material Table S1 for a complete list). Four NIST SRMs and 10 polymers that were sourced from scientific/laboratory vendors (scientifically sourced) were

considered the purest or best characterized. Raw materials obtained from manufacturers were considered purer than the consumer goods collected, which could contain additives. These standards represent each resin code #1 through #6, LLDPE, and several code #7 or other polymers (Table S1). The #7 category included polymers that could be found in marine debris, including acrylonitrile butadiene styrene (ABS), cellulose acetate (CA), ethylene vinyl acetate (EVA), latex, nitrile, nylon (represented by nylon 12 and nylon 6,6), polycarbonate (PC), poly (methyl methacrylate) (PMMA or acrylic), polytetrafluoroethylene (PTFE), fluorinated ethylene propylene (FEP), and polyurethane (PU).

Two to three consumer goods or raw materials labeled with each resin code were used to create standard spectra for each polymer. While consumer goods likely contain additives, the in-house spectral library was intentionally based on spectra from consumer goods, because they were assumed to more closely represent consumer items found in marine debris and ingested by marine organisms.

To validate the polymer identification by the analyst from ATR FT-IR spectra, eleven additional consumer goods with stamped resin codes were used in a blind test (Table S1): PETE ($n = 2$), HDPE ($n = 3$), LDPE ($n = 2$), PE of unknown density ($n = 1$), PP ($n = 2$), and PS ($n = 1$).

2.2. ATR FT-IR instrument details

A Perkin Elmer FT-IR Spectrometer Spectrum Two Universal ATR was used to collect spectra from 4000 cm^{-1} to 450 cm^{-1} with a data interval of 1 cm^{-1} . Resolution was set at 4 cm^{-1} . The ATR diamond crystal was cleaned with 70% 2-propanol and a background scan was performed between each sample. Each sample was compressed against the diamond with a force of at least 80 N to ensure good contact between sample and ATR crystal, as recommended by Perkin Elmer. Absorption bands identified using a peak height algorithm within the Perkin Elmer software were recorded and compared to absorption bands of each polymer reported in the literature and obtained from our in-house spectral library (Tables 1 and 2). A minimum of four matching absorption bands were required for accepted identification. Spectra of consumer goods of each polymer type tested are shown in Fig. 1. No pre-existing spectral library or database was used in this study. This was intentional, because comprehensive libraries can be expensive. We wanted our approach to be available to all labs regardless of their resources. Secondly, relying solely on automated library searches and statistical methods can lead to inaccurate identifications. For example, we suspect the automated approach used by Mecozzi et al. (2016) to identify plastic fragments from a sea turtle gastrointestinal tract resulted in inaccurate results. Three fragments were identified as polyethylene oxide, which is typically a liquid at environmental temperatures. Manual assessment of the spectra may have avoided this potential mistake.

We validated the ability to differentiate HDPE and LDPE via the relative intensity of a small absorption band at 1377 cm^{-1} , which represents the more abundant methyl group in highly branched LDPE (Asensio et al., 2009; Nishikida and Coates, 2003; Brandon et al., 2016). For samples determined to be PE, the spectral region of 1400 cm^{-1} to 1330 cm^{-1} was examined closely by magnifying this region in Microsoft Excel scatterplots. PE spectra were binned into the following seven categories in which 1377 cm^{-1} was 1) absent, 2) a shoulder on 1368 cm^{-1} , 3) a small bump on 1368 cm^{-1} , 4) the second largest band in this region, 5) nearly equal to 1368 cm^{-1} , 6) the strongest band in this region, 7) detected as a band by the instrument's software. The confidence of each bin to identify the PE type was assessed in three ways. Firstly, the ATR FT-IR spectral bin was recorded for each SRM, scientifically sourced or raw manufactured plastic standards of known PE. Secondly, the densities of PE standards and debris samples categorized across the bins were estimated via a float/sink test in different dilutions of ethanol (200 proof, A.C.S. reagent grade, Acros Organics, Fair Lawn, NJ) in deionized water. Dilutions were prepared volumetrically with graduated cylinders and ranged from 23% to 42% ethanol

with approximately 2% increments. Density of the solutions was measured by weighing 25 mL in a 25-mL graduated cylinder to the closest 0.0001 g. Relative standard uncertainty in measuring the density of these solutions was 0.34%. The measured densities of all PE standards and 49 PE marine debris pieces collected from Main Hawaiian Island beaches were used to assign the piece to either HDPE or LDPE based on known densities of these polymers (Peacock, 2000; Verleye et al., 2001). The percentage of HDPE or LDPE assignments via the float test within each bin provided quantified confidence in using each bin and allowed us to set clear criteria. Thirdly, tentative ATR FT-IR assignments of ingested plastics from sea turtles (samples described below; 5 HDPE and 5 LDPE) were confirmed with HT-SEC with differential refractive index, infrared, and multi-angle light scattering detection at NIST (methods described below).

Differentiation between LLDPE and LDPE was tested by examining the regions between 650 cm^{-1} and 1000 cm^{-1} . According to Nishikida and Coates (2003), absorbance bands at 890 cm^{-1} (vinylidene group) and 910 cm^{-1} (terminal vinyl group) should be of similar intensities and both weak for LLDPE, whereas they state that 890 cm^{-1} should be predominant in LDPE. These spectra regions from one scientifically sourced LLDPE and three consumer goods made of LLDPE were compared to several LDPE materials.

2.3. Ingested plastic collection

As described in Clukey et al. (2017), 2880 ingested plastic pieces were found in the gastrointestinal (GI) tracts of olive ridley ($n = 37$), green ($n = 9$), and loggerhead ($n = 4$) sea turtles caught incidentally by the Hawaiian and American Samoan longline fishery between 2012 and 2015. Pieces were removed with hexane-rinsed forceps, rinsed with nanopore deionized water, gently cleaned with cleanroom wipers, wrapped in hexane-rinsed foil, placed in a FEP bag, and archived frozen as part of the Biological and Environmental Monitoring and Archival of Sea Turtle tissues (BEMAST) project of the NIST Marine Environmental Specimen Bank (Keller et al., 2014).

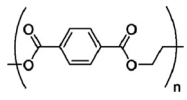
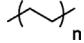
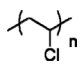
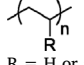
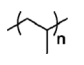
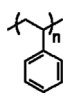
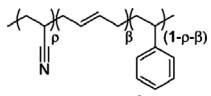
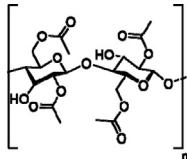
2.4. Plastic preparation

To minimize instrument time, a subset of pieces ($n = 828$) was selected for this study that visually represented all other pieces found in each turtle. A three-category rugosity scoring system was applied to some of the pieces and defined as (1) smooth, (2) ridged, and (3) rugose (Fig. S1). Pieces were weighed before and after FT-IR analysis, repackaged and frozen for continued archival storage by BEMAST and future chemical analysis.

Eleven plastic fragments ingested by olive ridley sea turtles were chosen for testing five different cleaning methods, after being identified using absorption bands in Table 1 as HDPE ($n = 3$), LDPE ($n = 5$), and PP ($n = 3$). These fragments were analyzed by ATR FT-IR after undergoing five different treatments: (1) no additional cleaning, (2) wiping a small area with a dry cleanroom wiper, (3) wiping a new area with a cleanroom wiper that was wet with 70% 2-propanol from a LDPE squirt bottle, (4) wiping a third area with a cleanroom wiper wet with deionized water from a LDPE squirt bottle, and (5) cutting the piece with hexane-rinsed scissors or pliers to expose the inside surface of the fragment. Three spectra were generated for each cleaning method on each piece by analyzing the fragment on three non-overlapping sections of the cleaned area. The optimal cleaning method was determined as described below in statistical methods. These less destructive cleaning methods were chosen over chemical manipulation with acids and strong solvents as in Mecozzi et al. (2016) for green chemistry reasons and to minimize manipulation so that the samples could be archived by BEMAST and tested in the future for persistent organic pollutants.

Table 1

List of important vibration modes and mode assignments for the ATR FT-IR spectra of eight of 16 polymers identified. The remaining eight polymers are in Table 2. Absorption bands listed are representative of vibrations critical for polymer identification. Please consult references for full lists of absorption bands.

Polymer	Resin code	Chemical structure	Absorption bands (cm ⁻¹) used for identification ^a	Assignment	Reference in addition to this study
Polyethylene terephthalate (PETE)	1		1713 (a) 1241 (b) 1094 (c) 720 (d)	C=O stretch C–O stretch C–O stretch Aromatic CH out-of-plane bend	Asensio et al., 2009; Verleye et al., 2001; Noda et al., 2007
High-density polyethylene (HDPE)	2		2915 (a) 2845 (b) 1472 (c) 1462 (d) 730 (e) 717 (f)	C–H stretch C–H stretch CH ₂ bend CH ₂ bend CH ₂ rock CH ₂ rock	Asensio et al., 2009; Noda et al., 2007; Nishikida and Coates, 2003
Polyvinyl chloride (PVC)	3		1427 (a) 1331 (b) 1255 (c) 1099 (d) 966 (e) 616 (f)	CH ₂ bend CH bend CH bend C–C stretch CH ₂ rock C–Cl stretch	Beltran and Marcilla, 1997; Verleye et al., 2001; Noda et al., 2007
Low-density polyethylene (LDPE) or linear LDPE (LLDPE)	4	 R = H or alkyl (LLDPE), PE (LDPE)	2915 (a) 2845 (b) 1467 (c) 1462 (d) 1377 (e) 730 (f) 717 (g)	C–H stretch C–H stretch CH ₂ bend CH ₂ bend CH ₃ bend CH ₂ rock CH ₂ rock	Asensio et al., 2009; Noda et al., 2007; Nishikida and Coates, 2003
Polypropylene (PP)	5		2950 (a) 2915 (b) 2838 (c) 1455 (d) 1377 (e) 1166 (f) 997 (g) 972 (h) 840 (i) 808 (j)	C–H stretch C–H stretch C–H stretch CH ₂ bend CH ₃ bend CH bend, CH ₃ rock, C–C stretch CH ₃ rock, CH ₃ bend, CH bend CH ₃ rock, C–C stretch CH ₂ rock, C–CH ₃ stretch CH ₂ rock, C–C stretch, C–CH stretch	Asensio et al., 2009; Verleye et al., 2001; Noda et al., 2007
Polystyrene (PS)	6		3024 (a) 2847 (b) 1601 (c) 1492 (d) 1451 (e) 1027 (f) 694 (g) 537 (h)	Aromatic C–H stretch C–H stretch Aromatic ring stretch Aromatic ring stretch CH ₂ bend Aromatic CH bend Aromatic CH out-of-plane bend Aromatic ring out-of-plane bend	Asensio et al., 2009; Verleye et al., 2001; Noda et al., 2007
Acrylonitrile butadiene styrene (ABS)	7	 ABS is mixture of <i>cis</i> , <i>trans</i> , and vinyl isomers, linear and crosslinked	2922 (a) 1602 (b) 1494 (c) 1452 (d) 966 (e) 759 (f) 698 (g)	C–H stretch Aromatic ring stretch Aromatic ring stretch CH ₂ bend =C–H bend Aromatic CH out-of-plane bend, =CH bend Aromatic CH out-of-plane bend	Verleye et al., 2001
Cellulose acetate (CA)	7		1743 (a) 1368 (b) 904 (c) 600 (d)	C=O stretch CH ₃ bend Aromatic ring stretch or CH bend O–H bend	Ilharco and Brito de Barros, 2000; Verleye et al., 2001; Noda et al., 2007

^a Resolution was 4 cm⁻¹. Letters can be cross referenced to bands shown in ATR FT-IR spectra in Fig. 1.

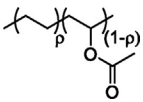
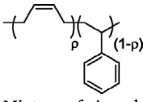
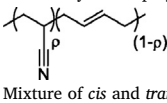
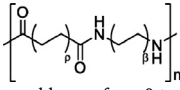
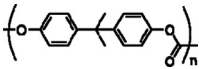
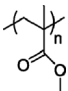
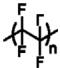
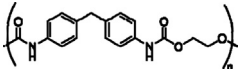
2.5. Analysis of ingested plastics for polymer type

The 828 ingested plastic pieces discovered in the turtles were analyzed by ATR FT-IR by first cleaning a small area with water and

cleanroom wiper or cutting to expose a smooth clean surface. Polymers were identified based on presence of absorption bands as described in Table 1 and shown in Fig. 1. Pieces producing absorption bands consistent with both PE and PP were assigned as “mixture” (Fig. 2). Pieces

Table 2

List of important vibration modes and mode assignments for the ATR FT-IR spectra for the remaining eight of 16 polymers identified. Absorption bands listed are representative of vibrations critical for polymer identification. Please consult references for full lists of absorption bands.

Polymer	Resin code	Chemical structure	Absorption bands (cm ⁻¹) used for identification ^a	Assignment	Reference in addition to this study
Ethylene vinyl acetate (EVA)	7		2917 (a) 2848 (b) 1740 (c) 1469 (d) 1241 (e) 1020 (f) 720 (g)	C–H stretch C–H stretch C=O stretch CH ₂ bend, CH ₃ bend C(=O)O stretch C–O stretch CH ₂ rock	Asensio et al., 2009; Verleye et al., 2001
Latex	7	 Mixture of <i>cis</i> and <i>trans</i> ; natural latex does not contain styrene copolymer	2960 (a) 2920 (b) 2855 (c) 1167 (d) 1447 (e) 1376 (f)	C–H stretch C–H stretch C–H stretch C=C stretch CH ₂ bend CH ₃ bend	Guidelli et al., 2011
Nitrile	7	 Mixture of <i>cis</i> and <i>trans</i>	2917 (a) 2849 (b) 2237 (c) 1605 (d) 1440 (e) 1360 (f) 1197 (g) 967 (h)	=C–H stretch =C–H stretch CN stretch C=C stretch CH ₂ bend CH ₂ bend CH ₂ bend =C–H bend	Coates, 2000; Verleye et al., 2001
Nylon (all polyamides)	7	 r and b vary from 0 to 12 based on monomer type	3298 (a) 2932 (b) 2858 (c) 1634 (d) 1538 (e) 1464 (f) 1372 (g) 1274 (h) 1199 (i) 687 (j)	N–H stretch CH stretch CH stretch C=O stretch NH bend, C–N stretch CH ₂ bend CH ₂ bend NH bend, C–N stretch CH ₂ bend NH bend, C=O bend	Rotter and Ishida, 1992; Verleye et al., 2001; Noda et al., 2007
Polycarbonate (PC)	7		2966 (a) 1768 (b) 1503 (c) 1409 (d) 1364 (e) 1186 (f) 1158 (g) 1013 (h) 828 (i)	CH stretch C=O stretch Aromatic ring stretch Aromatic ring stretch CH ₃ bend C–O stretch C–O stretch Aromatic CH in-plane bend Aromatic CH out-of-plane bend	Asensio et al., 2009; Verleye et al., 2001; Noda et al., 2007
Poly(methyl methacrylate) (PMMA or acrylic)	7		2992 (a) 2949 (b) 1721 (c) 1433 (d) 1386 (e) 1238 (f) 1189 (g) 1141 (h) 985 (i) 964 (j) 750 (k)	C–H stretch C–H stretch C=O stretch CH ₂ bend CH ₃ bend C–O stretch CH ₃ rock C–O stretch CH ₃ rock C–H bend CH ₂ rock, C=O bend	Verleye et al., 2001
Polytetrafluoroethylene (PTFE) or fluorinated ethylene propylene (FEP)	7		1201 (a) 1147 (b) 638 (d) 554 (e) 509 (f)	CF ₂ stretch CF ₂ stretch C–C–F bend CF ₂ bend CF ₂ bend	Coates, 2000; Verleye et al., 2001
Polyurethane (PU)	7		2865 (a) 1731 (b) 1531 (c) 1451 (d) 1223 (e)	C–H stretch C=O stretch C–N stretch CH ₂ bend C(=O)O stretch	Asefnejad et al., 2011; Verleye et al., 2001; Noda et al., 2007

^a Resolution was 4 cm⁻¹. Letters can be cross referenced to bands shown in ATR FT-IR spectra in [Fig. 1](#).

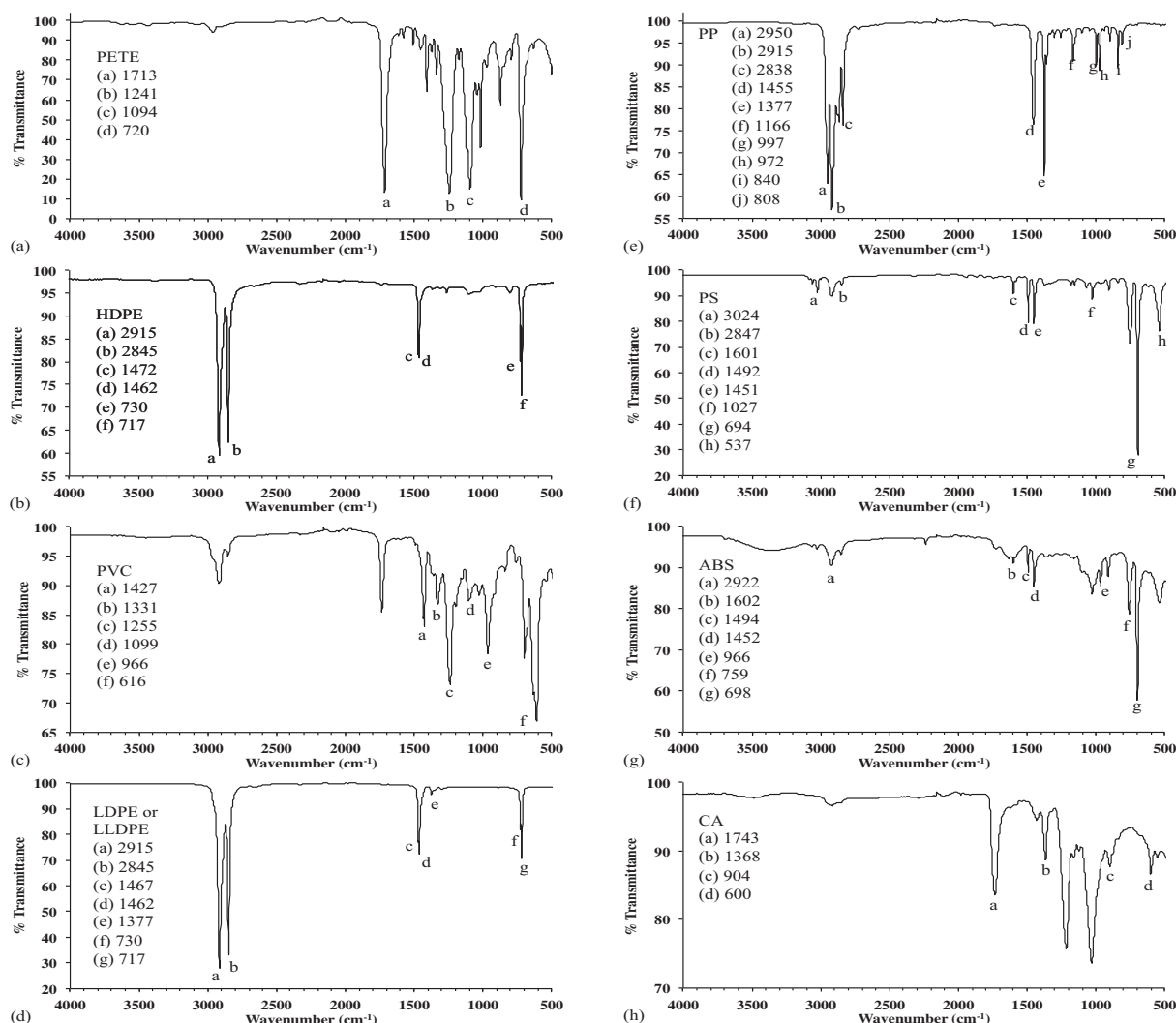


Fig. 1. Spectra produced from plastic consumer goods labeled with resin codes of (a) polyethylene terephthalate (PETE, #1), (b) high-density polyethylene (HDPE, #2), (c) polyvinyl chloride (PVC, #3), (d) low-density polyethylene and linear low density polyethylene (LDPE and LLDPE, #4), (e) polypropylene (PP, #5), and (f) polystyrene (PS, #6) along with ten other polymers: (g) acrylonitrile butadiene styrene (ABS), (h) cellulose acetate (CA), (i) ethylene vinyl acetate (EVA), (j) latex, (k) nitrile, (l) nylons, (m) polycarbonate (PC), (n) poly (methyl methacrylate) (PMMA), (o) polytetrafluoroethylene (PTFE) or fluorinated ethylene propylene (FEP), and (p) polyurethane (PU) using ATR FT-IR. Letters represent characteristic absorption bands (cm^{-1}) used to identify each polymer.

that could not be identified by ATR FT-IR spectra (e.g., presence of less than four identifying absorption bands) were assigned “unknown.” A subset of pieces that were identified by ATR FT-IR was analyzed by high HT-SEC with differential refractive index, infrared, and multi-angle light scattering detection.

Samples for HT-SEC were sonicated in ethanol for 10 min, followed by 10 min sonication in nanopure deionized water (18.2 MΩ) to remove aqueous soluble contaminants and minimize the addition of biological contaminants to the instrument. Approximately 10 mg of each sample was encased in a 5 μm stainless steel mesh and dissolved in HPLC grade 1,2,4-trichlorobenzene under nitrogen atmosphere for 1 h prior to injection in the instrument, allowing soluble polymers to dissolve and pass through the mesh, and insoluble debris, filler, or crosslinked components to remain sequestered in the mesh. The samples were injected into a Polymer Characterization (Valencia, Spain) GPC-IR instrument with an IR 4 detector consisting of two infrared IR detection bands, 2800 cm^{-1} to 3000 cm^{-1} representing the entire C–H stretching region (CH, CH_2 , and CH_3), and a narrow band at 2950 cm^{-1} for the methyl C–H stretch absorbances, respectively, as well as a Wyatt Technology (Santa Barbara, CA) Dawn Heleos II multi-angle light scattering (MALS) detector with 18 angles and a forward monitor (zero angle detector). Separately, the samples were also injected on a Tosoh

(Tokyo, Japan) HT-Eco SEC with differential refractive index detection. Both instruments ran at 160 $^{\circ}\text{C}$ with a 1,2,4-trichlorobenzene mobile phase with 300 ppm Irganox 1010 added as an antioxidant. The stationary phase columns used in both systems are a set of three Tosoh HT2 columns (two, Tosoh TSKgel GMHr-H (S) HT2, 13 μm mixed bed, 7.8 mm ID \times 30 cm columns and one, Tosoh TSKgel GMHr-H (20) HT2, 20 μm , 7.8 mm ID \times 30 cm column with an exclusion limit $\approx 4 \times 10^8$ g/mol). Sample molar masses, molar mass distribution, short chain branching content (SCB), were determined by calibration with narrow molar mass distribution PS standards, NIST SRM 1475a (linear, broad, HDPE), and NIST SRM 1478 (to determine inter-detector delay and normalize photodiode response of the MALS detector), and 10 blends of linear PE and PP with systematic variation of PP content, where the total degree of short chain branching (SCB) was confirmed by nuclear magnetic resonance spectroscopy (NMR). Calibration and data analysis was performed by proprietary software from each instrument vendor. HT-SEC and NMR have many advantages, but they can only measure polymer chains that are soluble under the solvent and temperature conditions used and they are not high-throughput like ATR-FTIR, which measures the bulk sample.

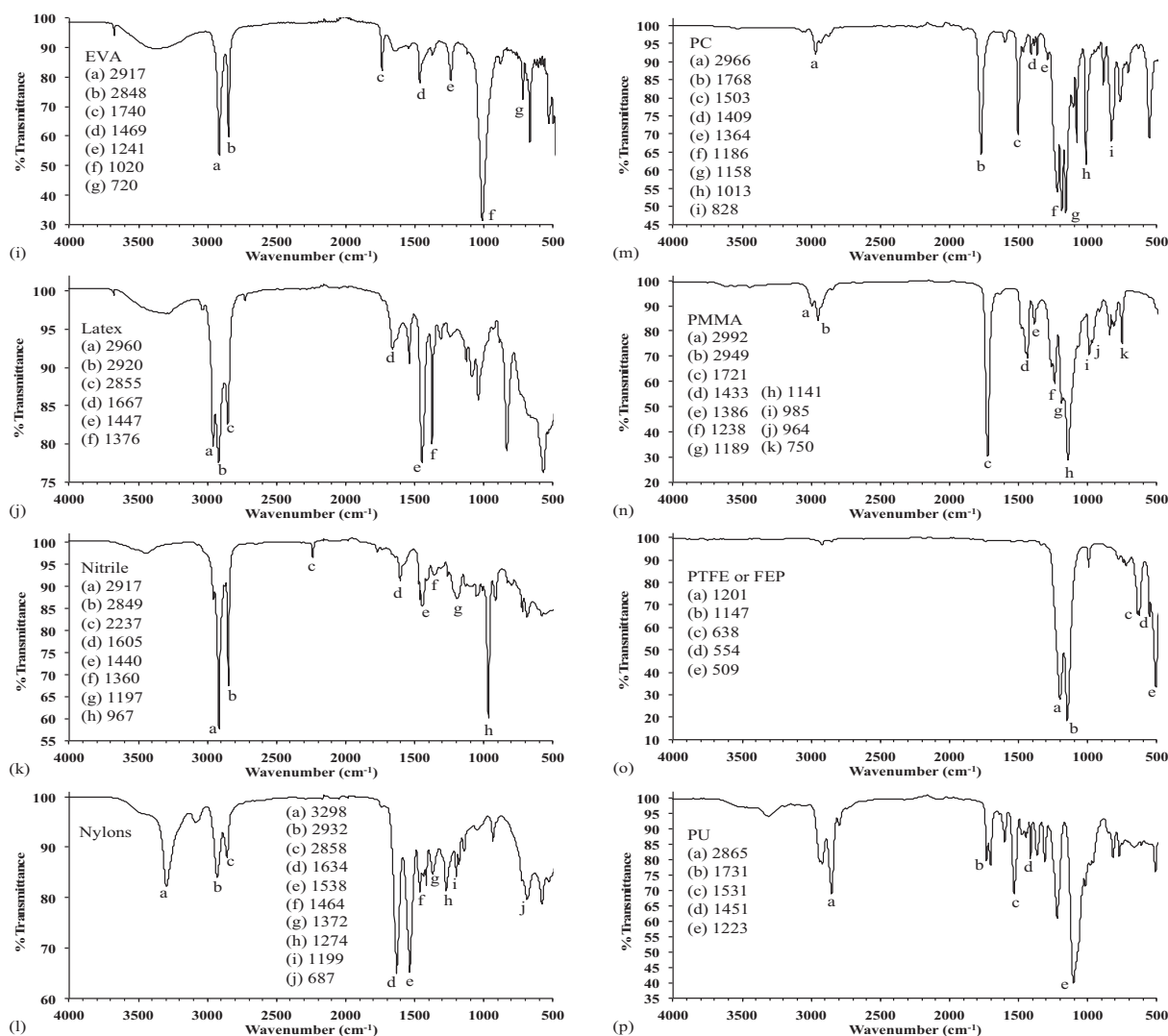


Fig. 1. (continued)

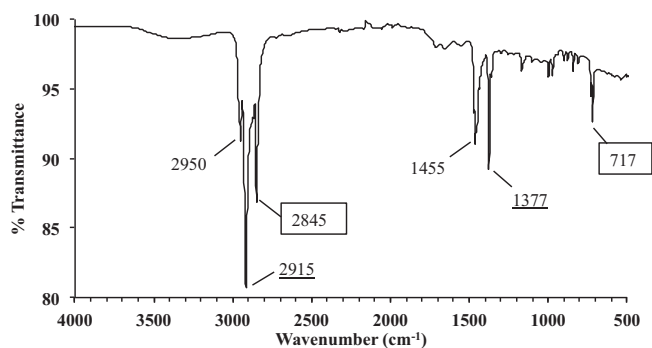


Fig. 2. ATR FT-IR spectrum of an ingested plastic fragment assigned as a mixture of polyethylene (PE) and polypropylene (PP). Wavenumbers in boxes are characteristic of PE, underlined wavenumbers are characteristic of both PE and PP, and unmarked wavenumbers are characteristic of PP.

2.6. Data handling and statistical analysis

Ordination was used to synthesize the absorbance data, in order to: 1) determine if novel absorption bands at additional wavenumbers could distinguish HDPE and LDPE, and 2) investigate if clustering of “unknown” ingested pieces near known polymers could help to identify their polymer composition. MetaboAnalyst software was used and the

“normalized by sum” option was chosen so that all spectral bands had equal weight and samples could be compared. Two principal component analyses (PCAs) were performed on different sample sets. PCA1 included spectra from three consumer goods of each of the following polymers: HDPE, LDPE, and PP. PCA2 included 797 ingested plastic pieces (793 identified, 4 unknown) of nine identified polymer types. Because PCA requires at least three samples of each polymer and less than three ingested pieces of PVC and nylon were discovered, it was necessary to include the spectra of consumer good items representing PVC and nylon in PCA2. PCA1 was run using bins of four wavenumbers over the entire spectral range of 4000 cm^{-1} to 450 cm^{-1} while PCA2 used selected absorption bands within a range of $\pm 1\text{ cm}^{-1}$ identified in Table 1 (plus additional bands from the literature) for polymers included in the analysis. All possible absorption bands were included in PCA1 to discover novel absorption bands for distinguishing HDPE from LDPE. No transformations were performed and Pareto scaling was used for both PCAs.

The optimal cleaning method was determined in two ways: 1) determining the percent of spectra that provided visually identifiable polymer assignment (good vs. poor quality spectra), and 2) counting the number of detectable absorption bands used for identification of that particular polymer. Wavenumbers with absorption bands greater than three times the noise surrounding the absorption band were recorded as detectable wavenumbers. All variables were tested for normality using the Shapiro-Wilk tests in IBM SPSS Statistics Version 24.

Because normality could not be accomplished even after data transformations, non-parametric Friedman's ANOVA tests followed by Wilcoxon signed-rank tests were used to compare differences in cleaning methods using two different response variables: percent of identifiable spectra and number of identifiable absorption bands greater than three times the noise. A Spearman Rank Order correlation was used to determine if rugosity had an effect on the number of detectable wavenumbers.

3. Results and discussion

3.1. ATR FT-IR polymer identification of consumer goods, raw manufactured, or scientifically sourced polymers

Plastic consumer goods from known resin codes produced spectra with expected absorption bands (Fig. 1, Table 1). When compared to the spectra of raw manufactured polymers or scientifically sourced polymers, the appearance and number of identifiable wavenumbers were nearly identical (data not shown). Absorption bands identified for these polymers were either a direct match or within four wavenumbers of the absorption bands listed in Table 1. Of the 18 polymers tested, all could be easily distinguished from each other with only three minor exceptions (Fig. 1). Spectra of FEP and PTFE showed absorbance bands at the same wavenumbers and with the same intensity for 638 cm^{-1} , 554 cm^{-1} , and 509 cm^{-1} , but the intensity of 1201 cm^{-1} (CF_2 stretch) and 1147 cm^{-1} (CF_2 stretch) were 16% and 27% higher, respectively, in PTFE than FEP. All types of nylon produced the same absorbance bands, so nylon-12 cannot be distinguished from nylon 6,6 or others (Verleye et al., 2001). Differentiating among HDPE, LLDPE, and LDPE is challenging, but our goal was to develop a simple ATR FT-IR method so that discrimination by sample destructive methods, such as HT-SEC with infrared detection or differential scanning calorimetry (DSC), is not required. Our results confirm that ATR FT-IR can identify consumer goods produced from PETE, PEs, PVC, PP, PS, ABS, CA, EVA, latex, nitrile, nylons, PC, PMMA, (PTFE or FEP), and PU, but PE samples require closer inspection of the ATR FT-IR spectra to distinguish HDPE from LDPE.

The use of ATR FT-IR for polymer identification was further confirmed via a blind test, in which 11 consumer goods consisting of diverse polymers were correctly identified by an analyst without prior knowledge of the resin code (Table S1). The five PE samples were all correctly identified as PE, but some could not be further categorized as either HDPE or LDPE. Of the three HDPE samples, one was correctly assigned and two were categorized as unknown PE. Of the two LDPE, one was correctly assigned and one was assigned unknown PE.

In hopes of discovering additional absorbance bands to distinguish HDPE from LDPE, a PCA was performed including the spectra of consumer goods of HDPE ($n = 3$), LDPE ($n = 3$), and PP ($n = 3$). The PCA showed no separation between HDPE and LDPE (Fig. S2). The first two principal components (PC) explained 78.3% of the variance and the loadings are shown in Table S2. This biplot revealed absorbance bands that differentiate PE from PP (700 cm^{-1} to 730 cm^{-1} , CH_2 rock), but no novel bands that could distinguish HDPE from LDPE (Fig. S2). While additional PCs explained more of the variation (14.7% by PC3 and 6% by PC4), they did not provide any additional separation of HDPE from LDPE. This is because HDPE and LDPE share the same major structural unit, functional groups, chemical bonds (Asensio et al., 2009), and therefore have many identical wavenumbers (Table 1). However, the different degree of branching results in small, but important differences, in the spectral region of 1400 cm^{-1} to 1330 cm^{-1} with LDPE having greater intensity at 1377 cm^{-1} due to methyl bending deformation of the branched chain ends (Asensio et al., 2009; Nishikida and Coates, 2003). This band may have been too small for the PCA to detect and must be magnified and compared to the intensity of 1368 cm^{-1} manually.

The differentiation between LDPE and HDPE with the presence of a

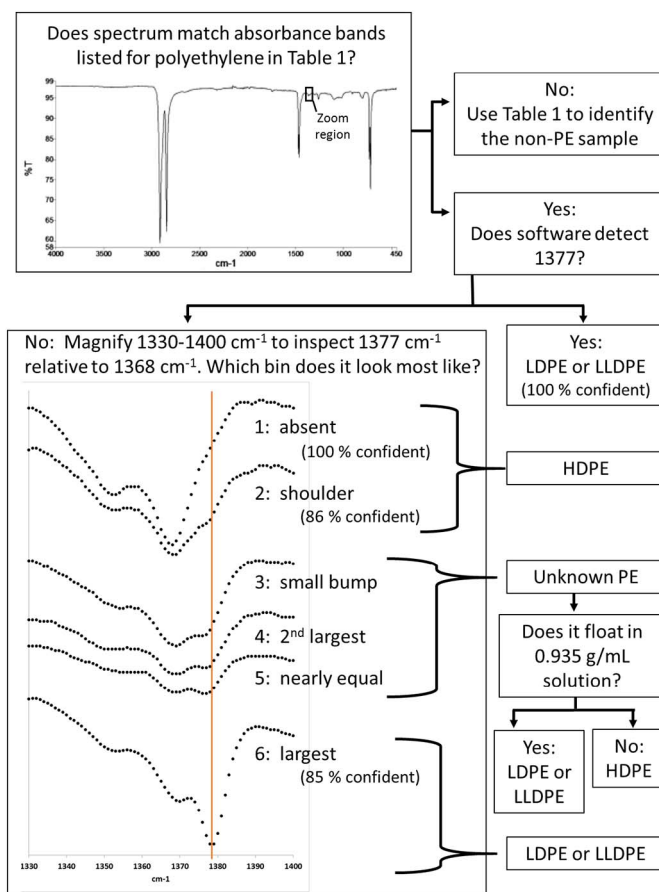


Fig. 3. Decision flow chart for differentiating high-density polyethylene (HDPE), linear low-density polyethylene (LLDPE), and low-density polyethylene (LDPE) using ATR FT-IR spectra and float/sink tests.

1377 cm^{-1} band is easy in some spectra, while others are more challenging. PE spectra fell into seven different bins based on the observation of the 1377 cm^{-1} band being: 1.) absent, 2.) a tiny shoulder, 3.) a small bump, 4.) the second largest in the 1400 cm^{-1} to 1330 cm^{-1} region, 5.) nearly equivalent to 1368 cm^{-1} band, 6.) the largest in this region, and 7.) detected by the instrument's software (Fig. 3). Bins at the extremes (1 and 2 are HDPE; 6 and 7 are LDPE) are clear, but those in the middle are ambiguous (bins 3, 4, and 5) and cause substantial confusion.

Table S1 describes ATR FT-IR results of each standard and consumer good tested. All but one of the SRMs, raw manufactured plastic or scientifically sourced standards of known PE ($n = 10$ for HDPE, $n = 4$ LLDPE, and $n = 17$ LDPE) were correctly and easily assigned because they fell in the clear bins (Table S1). One LDPE standard, SRM 1474b, fell into bin 3. Fourteen consumer good standards were stamped with HDPE ($n = 6$), LLDPE ($n = 3$), or LDPE ($n = 5$). Of these, eight (57%) were accurately assigned because they produced unambiguous spectra, six (43%) produced ambiguous spectra, and one (0.1%) with a clear spectrum was inaccurately assigned. Three of the six ambiguous samples were thin bags used for produce, shopping, and shipping. The incorrect standard was a grocery shopping bag stamped with #2 resin code (HDPE), but 1377 cm^{-1} was the strongest peak. These results suggest that thin sheet bags are consistently the most ambiguous and challenging to assign to HDPE versus LDPE for reasons currently unknown.

The other three ambiguous spectra came from all three LLDPE consumer goods tested. Because LLDPE has intermediate extents of branching, this was not surprising. Unfortunately, bins 3, 4, and 5 cannot be considered LLDPE, because materials known to be HDPE and

LDPE also produced spectra in these bins. A method to distinguish LLDPE from LDPE samples was proposed using another region of the spectra (650 cm^{-1} to 1000 cm^{-1}) by Nishikida and Coates (2003). They report that LLDPE should have equal and weak bands at 890 cm^{-1} (vinylidene group) and 910 cm^{-1} (terminal vinyl group), whereas 890 cm^{-1} is larger in LDPE. We could not confirm this method with a close examination of this spectral region with four LLDPE and 18 LDPE standards (Table S1). The four known LLDPE standards produced variable results. The LLDPE trash bag had equally weak bands, as expected. The LLDPE biohazard bag produced a band at 890 cm^{-1} was larger but nearly equal to the 910 cm^{-1} band. However, the scientifically sourced LLDPE sample produced no band at 890 cm^{-1} and a small band at 910 cm^{-1} , and the LLDPE tubing produced a larger band at 910 cm^{-1} than 890 cm^{-1} . As expected, 14 of the 18 LDPE samples (78%) produced a more intense 890 cm^{-1} band than 910 cm^{-1} . Three materials produced equally intense peaks (SRM 1476a, a swimmer's ear bottle, and a shipping bag), and for this reason we suspect they were produced with LLDPE. One produced a very small band at 910 cm^{-1} and no band at 890 cm^{-1} (a breastmilk storage bag). The inconsistent results within the known LLDPE standards did not give enough confidence to use this distinguishing method. Therefore, we conclude that LLDPE and LDPE cannot be distinguished from each other using ATR FT-IR.

In the ambiguous bins 3, 4, and 5, the 1377 cm^{-1} band appears as a small bump on the tail of the 1368 cm^{-1} band, a distinct but smaller band than 1368 cm^{-1} , or equivalent to the intensity of 1368 cm^{-1} , respectively. Confidence to assign these bins to a particular PE was assessed, for the first time to our knowledge, by estimating the density of PE samples using a float/sink test in different dilutions of ethanol. Using a graduated cylinder to volumetrically prepare solutions resulted in inaccuracies of solution densities of up to 0.02 g/mL . Because distinguishing between 0.93 g/mL and 0.94 g/mL required better accuracy, the density of the solutions was determined by weighing 25 mL in a graduated cylinder. Relative standard uncertainty in measuring the density of these solutions was 0.34% . Resulting estimated densities for each standard item are shown in Table S1. All PE standards that were not stamped or labeled with a resin code that were subsequently assigned LDPE because they fell in bins 6 and 7 ($n = 4$), floated in solutions $> 0.931\text{ g/mL}$ as expected. This added more confidence to our LDPE criteria. Furthermore, 19 of the 20 known LDPE or LLDPE standards (95%) tested had estimated densities of 0.938 g/mL or less; and all ten known HDPE standards had estimated densities of 0.938 g/mL or greater. Unexpectedly, one LDPE thin shipping bag sank in solutions up to 0.950 g/mL . Its greater density may be attributed to a silver-colored inner layer of unknown polymer composition.

Because our methods to differentiate HDPE from LDPE were slightly less successful in consumer goods than in raw or scientifically sourced standards, we confirmed our method using marine debris samples. Forty-nine plastic debris items collected from Main Hawaiian Island beaches that were discovered to be PE by ATR FT-IR were categorized as bin 1 ($n = 3$), bin 2 ($n = 14$), bin 3 ($n = 1$), bin 4 ($n = 5$), bin 5 ($n = 13$), and bin 6 ($n = 13$). These fragments were tested for floating or sinking in solutions with targeted densities of 0.935 g/mL and 0.941 g/mL . All of bin 1 samples sank, as expected for HDPE. 86% of bin 2 samples sank, providing enough confidence to conclude spectra with a shoulder at 1377 cm^{-1} are very likely HDPE. The one sample in bin 3 sank, suggesting samples producing a very small bump at 1377 cm^{-1} are HDPE, but our sample size was too small to have certainty. Only 40% of bin 4 and 46% of bin 5 floated in both solutions, suggesting these polymers could be either HDPE or LDPE when 1377 cm^{-1} is the second largest band or equivalent to 1368 cm^{-1} . 85% of bin 6 samples floated in both solutions, giving us enough confidence to confirm that spectra with 1377 cm^{-1} as the largest band are likely LDPE, even though the instrument's software does not detect it.

The inter-laboratory comparison using HT-SEC on PE ingested plastic samples, confirmed that ATR FT-IR assignments were 100%

Table 3

Comparison of identifications of ingested plastic samples analyzed by attenuated total reflectance Fourier transform infrared spectroscopy (ATR FT-IR) and high-temperature size exclusion chromatography (HT-SEC) with infrared, differential refractive index, and multi-angle light scattering detection.

HT-SEC results					
Identification by ATR FT-IR	Identification by HT-SEC	RI peak magnitude	Average $\text{CH}_3/1000$ total C ^a	Mn (kg/mol) ^c	Mw (kg/mol) ^c
PETE	PU ^b				
HDPE	HDPE	–	11.2 ± 7	1.1	36.2
HDPE	HDPE	–	10.6 ± 8	26.6	161.2
HDPE	HDPE	–	6.2 ± 9	6.0	83.8
HDPE	HDPE	–	9.9 ± 15	5.0	32.8
HDPE	HDPE	–	5.7 ± 9	15.2	80.4
LDPE	LDPE	–	24.0 ± 5	42.5	148.3
LDPE	LDPE	–	35.8 ± 17	0.9	70.9
LDPE	LDPE	–	48.3 ± 16	2.5	65.6
LDPE	LDPE	–	25.7 ± 9	32.0	148.4
LDPE	LDPE	–	54.7 ± 12	33.2	197.1
PP	PP	–	338.7 ± 6	42.4	196.4
PP	PP	–	348.4 ± 18	4.7	58.6
PP	PP	–	303.5 ± 5	6.8	44.5
PS	PS	+	15.2 ± 23	21.7	52.5
PS	PS	+	35.2 ± 27	28.2	557.2
PS	PS	+	34.1 ± 51	137.6	281.7

^a Represents the relative methyl content of the polymer across the measured molar mass distribution. Error represents one standard deviation of the methyl content across all molar masses measured. Precision of molar mass measurements is $\leq 5\%$ of reported value based on repeat injections of mass standards run during sample analyses.

^b Measured by XPS survey scan.

^c Polymer number average (Mn) and mass average (Mw) molar masses determined by MALS detection.

accurate (Table 3). These samples all produced unambiguous spectra ($n = 5$ HDPE, $n = 5$ LDPE). Taken together the results suggest there is a high confidence in unambiguous ATR FT-IR spectra to distinguish HDPE from LDPE. However, ambiguous spectra (bins 3–5) cannot be assigned to a particular PE polymer without further testing, and ATR FT-IR spectra cannot be used to distinguish LDPE from LLDPE. A detailed step-by-step decision tree outlines our criteria for distinguishing HDPE from LDPE using ATR FT-IR in addition to a float/sink test (Fig. 3). Once samples are determined to be PE based on absorbance bands listed in Table 1, the spectral region between 1330 cm^{-1} and 1400 cm^{-1} is magnified and each sample is matched to the most similar bin. Samples falling in bins 1 and 2 are assigned HDPE. Those in bins 3–5 are considered unknown PE until further testing can be done. Those in bins 6 and 7 are assigned LDPE or LLDPE. The unknown PE samples that are not air-filled can be placed into a 0.935 g/mL solution of ethanol. If they float, they are assigned LDPE or LLDPE. If they sink, they are assigned HDPE. The approach described in this decision tree should help future studies with the often confusing, yet very important, differentiation of HDPE and LDPE.

3.2. Cleaning methods for polymer identification of ingested plastics

To our knowledge, no study had addressed how digestive processes affect the FT-IR spectra of polymers, so we determined an optimal cleaning method that would also preserve the samples for future chemical testing. The spectra from the 11 ingested fragments after cleaning with water were of higher quality and easier to identify than before cleaning (Fig. S3), with the noise reduced and the absorbance bands more prominent. Thus, this test suggests that this simple treatment, involving removing surface residue with a cleanroom wiper and water, increases the ability to identify plastic polymers.

Only half of the spectra were of good enough quality to identify the polymer when no cleaning was performed on the samples ($58\% \pm 29\%$ standard deviation), whereas 100% of spectra were

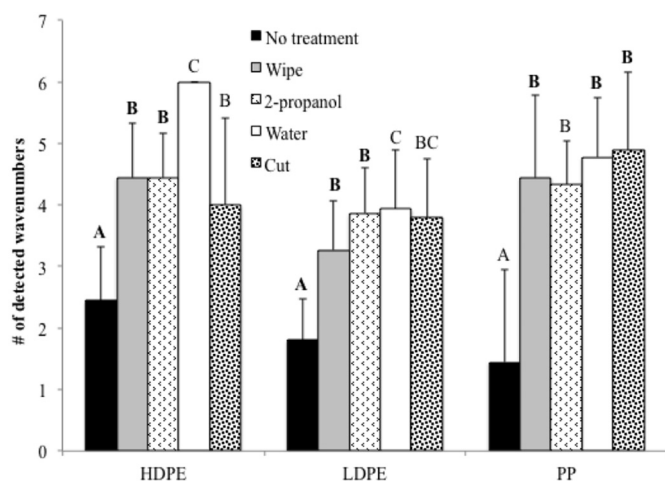


Fig. 4. Mean and standard deviation of the number of detected wavenumbers for five different cleaning methods on ingested high-density polyethylene (HDPE), low-density polyethylene (LDPE), and polypropylene (PP) fragments. Different letters above bars indicate significant differences among cleaning techniques within a polymer type ($p < 0.05$ Wilcoxon signed-rank tests).

identifiable with the other four cleaning methods (Fig. S4). Significant differences in the percent of spectra that could be identified were found among the five cleaning methods (Friedman's analysis of variance (ANOVA), $\chi^2(4) = 26.20$, $p < 0.0001$, $n = 11$). Post-hoc comparisons using Wilcoxon signed-rank tests revealed that all four sample treatments (wiping ($p = 0.004$, $n = 11$), cleaning with 2-propanol ($p = 0.004$, $n = 11$), water ($p = 0.004$, $n = 11$), or cutting ($p = 0.004$, $n = 11$)) resulted in a greater percentage of the spectra being identified, when compared to no cleaning (Fig. S4). No significant differences were found among the four cleaning methods. These results suggest that cleaning a polymer of ingested plastic fragments with any of the four methods should improve quality of ATR FT-IR spectra.

The number of detected peaks increased significantly for all three polymer types after performing any of the four cleaning methods (Fig. 4). The number of detected peaks and rugosity codes for each cleaning method for each fragment can be found in Table S3. Significant differences were found among the five cleaning methods for HDPE (Friedman's ANOVAs, $\chi^2(4) = 27.41$, $p < 0.0001$), for LDPE ($\chi^2(4) = 34.992$, $p < 0.0001$) and for PP ($\chi^2(4) = 19.92$, $p = 0.001$). For HDPE, wiping (Wilcoxon $p = 0.007$), 2-propanol ($p = 0.006$), water ($p = 0.005$), and cutting ($p = 0.018$) produced significantly more detectable peaks than no treatment. Cleaning HDPE fragments with water also produced significantly more detectable peaks when compared to wiping ($p = 0.008$), 2-propanol ($p = 0.008$), and cutting ($p = 0.014$). Similar results were seen with PP and LDPE ingested fragments (Fig. 4). These differences suggest that cleaning the surface of ingested fragments with water will produce the spectrum with the most detectable peaks and this method might be preferred if the goal is to minimize handling so that the pieces can be used in the future for additional chemical testing, such as measuring sorbed persistent organic pollutants.

LDPE fragments with a higher rugosity code yielded fewer detectable peaks ($r_s = -0.803$, $n = 5$, $p = 0.102$), although the relationship was not significant (Fig. S5). In contrast, when fragments were cut, no significant correlation was found between the number of detectable peaks and rugosity codes ($r_s = 0.631$, $n = 5$, $p = 0.254$). This is most likely due to rugosity being reduced when a fragment is cut. Therefore, if a rugose fragment cannot be identified after being cleaned with water, cutting may be the most effective cleaning method as it can allow for the sample to come in more direct contact with the diamond and thus evanescent wave, resulting in more detectable peaks.

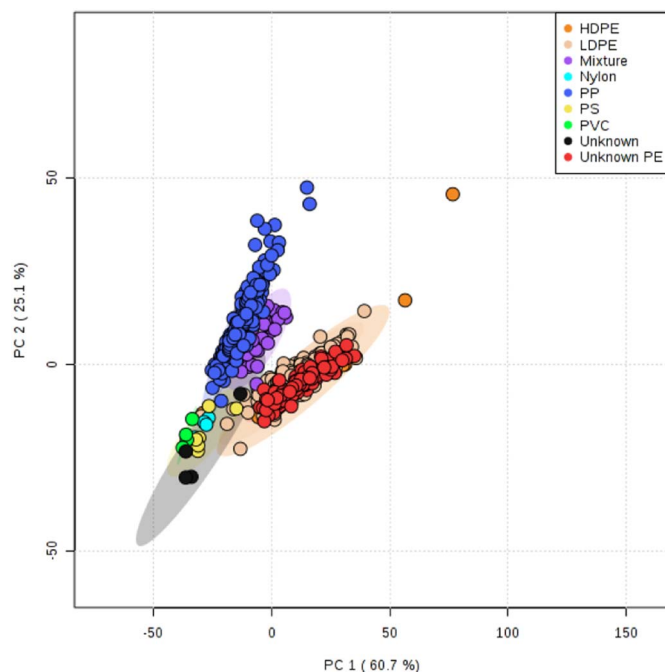


Fig. 5. PCA ordination of spectra from ingested plastic samples identified as high-density polyethylene (HDPE, $n = 58$), polyvinyl chloride (PVC, $n = 1$), low-density polyethylene (LDPE, $n = 310$), polypropylene (PP, $n = 270$), polystyrene (PS, $n = 7$), nylon ($n = 1$), PE/PP mixture ($n = 40$), unknown PE ($n = 106$), and unknown ($n = 4$). Spectra of consumer good items representing PVC ($n = 3$) and nylon ($n = 3$) were also included. The amount of variation in the data explained by each principal component is shown in parentheses.

3.3. Method validation with ingested polymers

Only 30 of the 828 ingested plastic pieces analyzed (4%) produced spectra of poor quality that could not be identified by ATR FT-IR. Criteria for differentiating HDPE and LDPE (even without the float/sink test, which was not applied to these samples) allowed assignment of 77.7% of the PE pieces, while 22.3% of PE samples fell in the unknown PE category. This proportion is similar to the 70% assignment capability of oceanic microplastics by Brandon et al. (2016).

PCA was performed on spectra from 797 representative ingested plastic pieces identified as HDPE ($n = 58$), PVC ($n = 1$), LDPE or LLDPE ($n = 310$; one outlier was removed), PP ($n = 270$; one outlier was removed), PS ($n = 7$), nylon ($n = 1$), mixture of PP and PE ($n = 40$), unknown PE ($n = 106$) and unknown ($n = 4$) along with plastic consumer goods of PVC and nylon. The PCA shows distinction between PEs and PP (Fig. 5; Table S4 for loadings) with 85.8% of the variance explained within the first two principal components. In an earlier version of the PCA, more of the ingested pieces, a total of 10, were originally identified as unknown (data not shown). The clustering of six of the unknown samples within the PCA, followed by further review of their ATR FT-IR spectra, allowed polymer assignment of these samples. These results suggest that PCA is a tool that can help interpret ambiguous spectra. Plastic pieces identified as a mixture were located between clusters for PE and PP as expected. In order to improve assignment of these predominantly olefinic polymers, HT-SEC with multiple detectors was used to definitively identify the samples as a mixture of PE and PP, and confirm results of the PCA.

Sixteen of 17 ingested plastic samples were positively identified by HT-SEC. All HT-SEC determined identities matched those obtained by ATR FT-IR, as shown in Table 3. Example chromatograms for three samples, identified as PS, LDPE, and HDPE are shown in Fig. 6. A number of qualitative and quantitative pieces of information were used to identify the polymers analyzed by HT-SEC. First, the injected polymer samples demonstrated a positive or negative differential

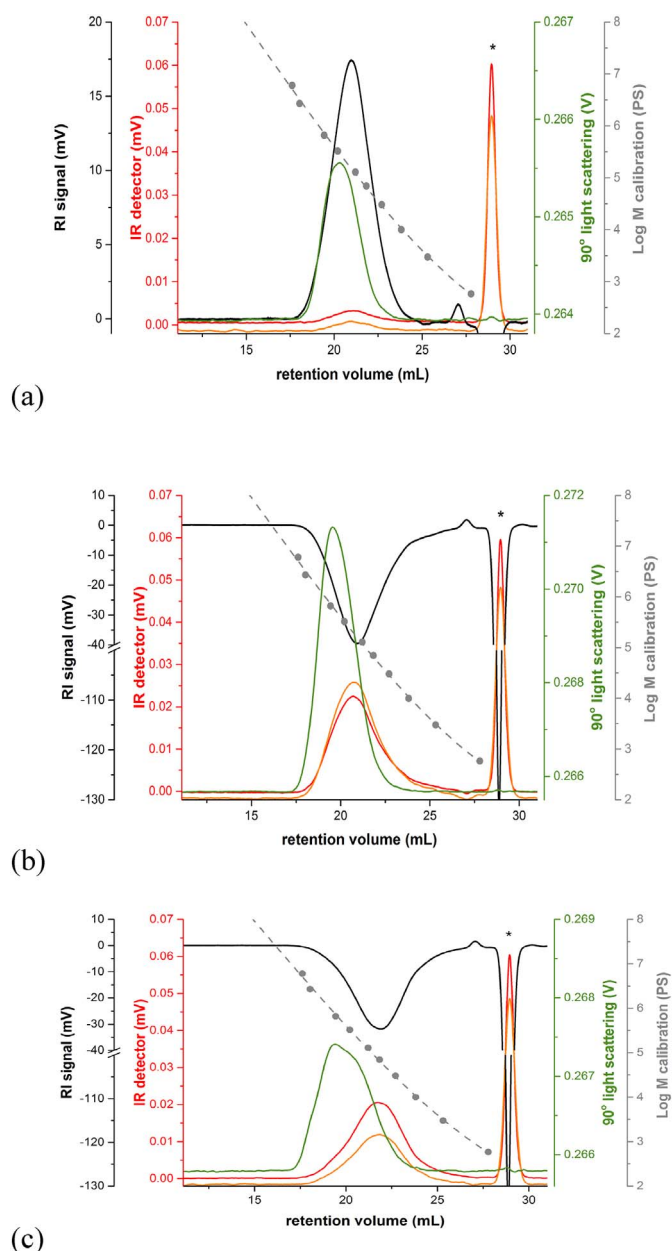


Fig. 6. Representative HT-SEC chromatograms of samples run to confirm ATR-FTIR materials for ingested samples identified as (a) polystyrene (PS) (b) low-density polyethylene (LDPE) (c) high-density polyethylene (HDPE). The $\text{CH}_3/1000$ total C were measured by the ratio of the two IR signals, methyl stretching bands and alkyl stretching bands at 2950 cm^{-1} and $(2800\text{ to }3000)\text{ cm}^{-1}$ (broad detector range), being represented by the orange and red traces, respectively. The asterisk (*) denotes an added flow rate marker, dodecane, used as an internal standard. (For interpretation of the references to color in this figure legend, the reader is referred to the web version of this article.)

refractive index (RI) peak as they eluted from the columns, indicative that the polymer had a greater or lesser refractive index than the mobile phase ($n_0 = 1.56$). Refractive indices of commercial polymers are available from a number of sources (Brandrup et al., 1999; Mark, 2007). This qualitative identification is used to rule out general classes of polymers; for example, polyolefins (PP, HDPE, LDPE) have a refractive index < 1.56 , so these polymers must have a negative RI elution peak (Table 3, Fig. 6b and c).

Differentiation between PP, HDPE, and LDPE was based on the degree of short chain branching, which was measured using the HT-SEC IR detector. The flow-through IR detector measures alkyl and methyl C–H stretching simultaneously as the separated polymer elutes. The

ratio of the two absorption spectra at each elution volume (Fig. 6), when compared to a calibration curve, permit branching content to be determined across the molar mass distribution. As ATR FT-IR is a bulk measurement, the branching content measured by HT-SEC was averaged across the molar mass distribution for each sample and the average methyl content per 1000 total carbons ($\text{CH}_3/1000$ total C) is shown in Table 3. HDPE is identified from samples that have 10 $\text{CH}_3/1000$ total C or less, as the only CH_3 contributions in HDPE are from chain ends, which are negligible. This is also a convenient metric as the limit of detection for the IR detector is 10 $\text{CH}_3/1000$ total C. PP was identified for polymers with a methyl content of $(330 \pm 33)\text{ CH}_3/1000$ total C, which is determined from theoretical calculations based on the propylene repeat unit. The 10% tolerance is to include PP that may have some small degrees of degradation from the turtle digestive tract as well as account for small variations ($< 10\%$) that were observed in HT-SEC analysis of consumer-grade PP (stamped resin code 5) when compared to reagent grade PP obtained from Sigma Aldrich. Currently, there is no documentary standard that specifies what purity a consumer polymer must have to be stamped with a specific resin code. LDPE is assigned to polymers with an average branching content between HDPE and PP, or (10 to 300) $\text{CH}_3/1000$ total C. For the purposes of this study, no effort was made to distinguish LLDPE from LDPE in ingested plastics, as ATR FT-IR cannot make that distinction. Future studies will address distinguishing LLDPE from LDPE in unknown polymer samples and mixtures with the addition of a differential viscometer to measure long chain branching.

Three of the 17 samples were identified as PS (Fig. 6a) based on several lines of evidence. Their positive differential RI signal and minimal alkyl content lead to small IR peak areas and large standard deviations in $\text{CH}_3/1000$ total C determinations. Also, there was agreement between polymer number average (M_n) and mass average (M_w) molar masses determined by MALS (considered an absolute measurement technique) and those determined by relative comparison to polystyrene standards. M_n and M_w values were determined for all samples and are listed as information values in Table 3.

One sample measured by HT-SEC (assigned as PETE by ATR FT-IR) was completely insoluble in 1,2,4-trichlorobenzene at 160°C , and no peaks were not observed in HT-SEC chromatograms using any detector. The second independent assignment of this sample was instead based on survey x-ray photoelectron spectroscopy (XPS) to measure the elemental composition in the sample. Elemental composition of this sample was $(80.3 \pm 0.9)\%$ C, $(3.6 \pm 0.3)\%$ N, and $(15.0 \pm 0.9)\%$ O, plus additional trace elements (silica and calcium and sodium salts), taken as an average of three locations on the sample. A tentative assignment of PU was made on the material, as the carbon, nitrogen, and oxygen content was closest to database values for PU at 78.6%, 8.4%, and 14%, respectively. As XPS only excites photoelectrons within the first $\approx 10\text{ nm}$ of a material, further sampling and measurements of the material will have to be performed. While this piece of brown fabric produced an ATR FT-IR spectrum with six absorption bands matching PETE, it was a poor-quality spectrum. XPS database values for PETE are 68.9% carbon, 31.1% oxygen, and do not contain nitrogen, which are generally more different from the readings of this fabric piece than those of PU. Taking all data into account, this piece was assigned PU.

With the exception of one misidentification, these novel inter-laboratory results support using ATR FT-IR to identify polymers of degraded and ingested plastics. Identifying the polymers comprising ingested plastic using this simple, accurate method can help us understand many aspects of the marine debris problem. The polymer type will dictate the transport and fate of marine debris and its affinity for other chemical pollutants. Furthermore, knowing the predominant polymer can inform better conservation and management practices. For example, LDPE and PP (resin code #4 and #5) represent large proportions of marine debris and are not commonly recycled in the Hawaiian Islands. Incentive programs for recycling these polymers and innovative post-use applications could be prioritized to help reduce the

abundance of LDPE and PP in the marine environment.

4. Conclusion

As the ingestion of plastic debris by threatened marine species such as sea turtles increases, the need to categorize plastic debris by polymer type and identify marine transport mechanisms and fates has become a high research priority. Here, we provide a definitive validation of ATR FT-IR to identify ingested plastic polymer types, including resin codes #1 through #6 and many polymers within code #7 without the use of a costly database. A clear, easy to follow guide of thoroughly tested criteria was presented to confidently differentiate HDPE and LDPE. Our approach has been successfully used by four additional ongoing marine debris studies with macro to microplastics found in water, on beaches, or ingested by other marine organisms. We encourage future studies to prepare ingested plastic samples by cleaning them with water or cutting rugose pieces to get a clean surface prior to ATR FT-IR analysis to produce the most accurate results. PCA can be leveraged to assign polymer types to the small proportion of pieces that present challenging ATR FT-IR spectra. This method has been used to identify the polymer composition ingested by three species of sea turtles in the pelagic Pacific. Results on polymers ingested by sea turtle species, geographical, and other comparisons will be reported in a forthcoming manuscript (Jung, 2017). The data reported in the current method development study represent only selected pieces; therefore, calculating the percentage of each polymer reported here would misrepresent the actual ingested composition.

The accuracy of using ATR FT-IR for identifying commercial polymers in marine debris, as demonstrated in this study, has the benefit of rapid analysis and minimal destruction to the collected samples, which is ideal for high throughput analysis of large repositories of marine debris. There is, however, much more detailed information about discarded plastics that can be explored by utilizing advanced polymer metrology methods, such as HT-SEC, thermal analysis, or rheological measurements. Systematic changes in chemical composition, molar mass, molar mass distribution and viscoelastic properties in a specific polymeric resin can provide better understanding of material degradation pathways and resulting byproducts. Comprehensive understanding of the origins, transport, fate, and lifetime of marine debris will ultimately require both high-throughput and fundamental studies of discarded materials, providing ample opportunities for collaboration between the life sciences and material science communities to address the challenges in marine plastics moving forward.

Disclaimer

Certain commercial equipment, instruments, or materials are identified in this paper to specify adequately the experimental procedure. Such identification does not imply recommendation or endorsement by the National Institute of Standards and Technology, nor does it imply that the materials or equipment identified are necessarily the best available for the purpose.

Acknowledgements

Funding was provided by grant 60NANB15D026 from the U.S. Pacific Islands Program of the NIST Marine Environmental Specimen Bank. The ATR FT-IR instrument was supported by National Institutes of Health grant P20GM103466. We thank Stacy (Vander Pol) Schuur for providing some of the raw manufactured polymers. We thank Tracy Schock for her advice on principal component analyses. We thank the fishermen and fisheries observers for carefully assessing, storing, and transporting the sea turtle specimens. We thank Shandell Brunson, Irene Nurzia Humburg, Devon Franke, Emily Walker, Sarah Alessi, T. Todd Jones (PIFSC), Bob Rameyer (USGS), Katherine Clukey, Jessica Jacob, Frannie Nilsen, Julia Smith, Adam Kurtz, Angela Hansen,

Stephanie Shaw, Jennette VanderJagt, and Jessica Kent (Hawaii Pacific University) and numerous other volunteers for help in sample collection and processing. We thank the entire NIST Marine Environmental Specimen Bank team, especially Rebecca Pugh and Paul Becker, for sample archival. Finally, we thank Chris Stafford, Amanda Forster and Rebecca Pugh for comments on the draft manuscript. Mention of products and trade names does not imply endorsement by the U.S. Government.

Appendix A. Supplementary data

Supplementary data to this article can be found online at <https://doi.org/10.1016/j.marpolbul.2017.12.061>.

References

- Andrady, A.L., 2011. Microplastics in the marine environment. *Mar. Pollut. Bull.* 62 (8), 1596–1605.
- Andrady, A.L., 2017. The plastic in microplastics: a review. *Mar. Pollut. Bull.* 119 (1), 12–22.
- Asefnejad, A., Khorasani, M.T., Behnamghader, A., Farsadzadeh, B., Bonakdar, S., 2011. Manufacturing of biodegradable polyurethane scaffolds based on polycaprolactone using a phase separation method: physical properties and in vitro assay. *Int. J. Nanomedicine* 6, 2375.
- Asensio, R.C., Moya, M.S.A., de la Roja, J.M., Gómez, M., 2009. Analytical characterization of polymers used in conservation and restoration by ATR-FTIR spectroscopy. *Anal. Bioanal. Chem.* 395 (7), 2081–2096.
- ASTM International, 2013. Standard Practice for Coding Plastic Manufactured Articles for Resin Identification. Designation: D7611/D7611M – 13^{e1}.
- Bakir, A., Rowland, S.J., Thompson, R.C., 2014. Enhanced desorption of persistent organic pollutants from microplastics under simulated physiological conditions. *Environ. Pollut.* 185, 16–23.
- Beltran, M., Marcilla, A., 1997. Fourier transform infrared spectroscopy applied to the study of PVC decomposition. *Eur. Polym. J.* 33 (7), 1135–1142.
- Bjorndal, K.A., Bolten, A.B., Lagueux, C.J., 1994. Ingestion of marine debris by juvenile sea turtles in coastal Florida habitats. *Mar. Pollut. Bull.* 28 (3), 154–158.
- Brandon, J., Goldstein, M., Ohman, M.D., 2016. Long-term aging and degradation of microplastic particles: comparing in situ oceanic and experimental weathering patterns. *Mar. Pollut. Bull.* 110 (1), 299–308.
- Brandrup, J., Immergut, E.H., Grulke, E.A., 1999. *Polymer Handbook*, Fourth Edition. John Wiley & Sons, Inc., New York, pp. 2336.
- Bugoni, L., Krause, L., Petry, M.V., 2001. Marine debris and human impacts on sea turtles in southern Brazil. *Mar. Pollut. Bull.* 42 (12), 1330–1334.
- Cincinelli, A., Scopetani, C., Chelazzi, D., Lombardini, E., Martellini, T., Katsoyiannis, A., Fossi, M.C., Corsolini, S., 2017. Microplastic in the surface waters of the Ross Sea (Antarctica): occurrence, distribution and characterization by FTIR. *Chemosphere* 175, 391–400.
- Clukey, K.E., Lepczyk, C.A., Balazs, G.H., Work, T.M., Lynch, J.M., 2017. Investigation of plastic debris ingestion by four species of sea turtles collected as bycatch in pelagic Pacific longline fisheries. *Mar. Pollut. Bull.* 120 (1–2), 117–125.
- Coates, J., 2000. Interpretation of infrared spectra, a practical approach. In: Meyers, R.A. (Ed.), *Encyclopedia of Analytical Chemistry*. John Wiley & Sons, Ltd., Chichester, pp. 10815–10837.
- Cole, M., Galloway, T.S., 2015. Ingestion of nanoplastics and microplastics by Pacific oyster larvae. *Environ. Sci. Technol.* 49 (24), 14625–14632.
- Cole, M., Webb, H., Lindeque, P.K., Fileman, E.S., Halsband, C., Galloway, T.S., 2014. Isolation of microplastics in biota-rich seawater samples and marine organisms. *Sci. Rep.* 4, 4528.
- Dümichen, E., Barthel, A.K., Braun, U., Bannick, C.G., Brand, K., Jekel, M., Senz, R., 2015. Analysis of polyethylene microplastics in environmental samples, using a thermal decomposition method. *Water Res.* 85, 451–457.
- Endo, S., Takizawa, R., Okuda, K., Takada, H., Chiba, K., Kanehiro, H., Ogi, H., Yamashita, R., Date, T., 2005. Concentration of polychlorinated biphenyls (PCBs) in beached resin pellets: variability among individual particles and regional differences. *Mar. Pollut. Bull.* 50 (10), 1103–1114.
- Fischer, M., Scholz-Böttcher, B.M., 2017. Simultaneous trace identification and quantification of common types of microplastics in environmental samples by pyrolysis-gas chromatography-mass spectrometry. *Environ. Sci. Technol.* 51 (9), 5052.
- Frère, L., Paul-Pont, I., Moreau, J., Soudant, P., Lambert, C., Huvet, A., Rinnert, E., 2016. A semi-automated Raman micro-spectroscopy method for morphological and chemical characterizations of microplastic litter. *Mar. Pollut. Bull.* 113 (1), 461–468.
- Fries, E., Zarfl, C., 2012. Sorption of polycyclic aromatic hydrocarbons (PAHs) to low and high density polyethylene (PE). *Environ. Sci. Pollut. Res.* 19 (4), 1296–1304.
- Geyer, R., Jambeck, J.R., Law, K.L., 2017. Production, use, and fate of all plastics ever made. *Sci. Adv.* 3 (7), e1700782.
- Guidelli, E.J., Ramos, A.P., Zaniquelli, M.E.D., Baffa, O., 2011. Green synthesis of colloidal silver nanoparticles using natural rubber latex extracted from *Hevea brasiliensis*. *Spectrochim. Acta A Mol. Biomol. Spectrosc.* 82 (1), 140–145.
- Hoarau, L., Ainley, L., Jean, C., Ciccione, S., 2014. Ingestion and defecation of marine debris by loggerhead sea turtles, *Caretta caretta*, from by-catches in the South-West Indian Ocean. *Mar. Pollut. Bull.* 84 (1), 90–96.

- Hoss, D.E., Settle, L.R., 1990. Ingestion of plastics by teleost fishes. In: Proceedings of the Second International Conference on Marine Debris. NOAA Technical Memorandum. NOAA-TM-NMFS-SWFS-154. Miami, FL, pp. 693–709.
- Howell, E.A., Bograd, S.J., Morishige, C., Seki, M.P., Polovina, J.J., 2012. On North Pacific circulation and associated marine debris concentration. *Mar. Pollut. Bull.* 65 (1), 16–22.
- Ilharco, L.M., Brito de Barros, R., 2000. Aggregation of pseudoisocyanine iodide in cellulose acetate films: structural characterization by FTIR. *Langmuir* 16 (24), 9331–9337.
- Jambeck, J.R., Geyer, R., Wilcox, C., Siegler, T.R., Perryman, M., Andrady, A., Narayan, R., Law, K.L., 2015. Plastic waste inputs from land into the ocean. *Science* 347 (6223), 768–771.
- Jung, M., 2017. Polymer Identification of Plastic Debris Ingested by Pelagic-phase Sea Turtles in the Central Pacific (Master Thesis). Hawaii Pacific University, Kaneohe, HI.
- Keller, J.M., Pugh, R.S., Becker, P.R., 2014. Biological and environmental monitoring and archive of sea turtle tissues (BEMAST): rationale, protocols, and initial collections of banked sea turtle tissues. In: NIST Internal Report (NISTIR)-7996.
- Koelmans, A.A., Besseling, E., Wegner, A., Foekema, E.M., 2013. Plastic as a carrier of POPs to aquatic organisms: a model analysis. *Environ. Sci. Technol.* 47 (14), 7812–7820.
- Mark, J.E. (Ed.), 2007. *Physical Properties of Polymers Handbook*. vol. 1076 Springer, New York.
- McIlgorm, A., Campbell, H.F., Rule, M.J., 2011. The economic cost and control of marine debris damage in the Asia-Pacific region. *Ocean Coast. Manag.* 54 (9), 643–651.
- Mecozzi, M., Pietroletti, M., Monakhova, Y.B., 2016. FTIR spectroscopy supported by statistical techniques for the structural characterization of plastic debris in the marine environment: application to monitoring studies. *Mar. Pollut. Bull.* 106 (1), 155–161.
- Moore, C.J., Moore, S.L., Leecaster, M.K., Weisberg, S.B., 2001. A comparison of plastic and plankton in the North Pacific central gyre. *Mar. Pollut. Bull.* 42 (12), 1297–1300.
- Nelms, S.E., Duncan, E.M., Broderick, A.C., Galloway, T.S., Godfrey, M.H., Hamann, M., Lindeque, P.K., Godley, B.J., 2015. Plastic and marine turtles: a review and call for research. *ICES J. Mar. Sci.* 73 (2), 165–181.
- Nilsen, F., Hyrenbach, K.D., Fang, J., Jensen, B., 2014. Use of indicator chemicals to characterize the plastic fragments ingested by Laysan albatross. *Mar. Pollut. Bull.* 87 (1), 230–236.
- Nishikida, K., Coates, J., 2003. Infrared and Raman analysis of polymers. In: Lobo, H., Bonilla, J.V. (Eds.), *Handbook of Plastics Analysis*. Marcel Dekker, Inc, New York, pp. 186–316.
- Noda, I., Dowrey, A.E., Haynes, J.L., Marcott, C., 2007. Group frequency assignments for major infrared bands observed in common synthetic polymers. In: Mark, J.E. (Ed.), *Physical Properties of Polymers Handbook*. Springer Science + Business Media, LLC, New York, pp. 395–406.
- Peacock, A., 2000. *Handbook of Polyethylene: Structures, Properties, and Applications*. Marcel Dekker, Inc., New York, pp. 534.
- Provencher, J.F., Bond, A.L., Avery-Gomm, S., Borrelle, S.B., Rebolledo, E.L.B., Hammer, S., Kühn, S., Lavers, J.L., Mallory, M.L., Trevail, A., van Franeker, J.A., 2017. Quantifying ingested debris in marine megafauna: a review and recommendations for standardization. *Anal. Methods* 9 (9), 1454–1469.
- Rios, L.M., Moore, C., Jones, P.R., 2007. Persistent organic pollutants carried by synthetic polymers in the ocean environment. *Mar. Pollut. Bull.* 54 (8), 1230–1237.
- Rochman, C.M., Hoh, E., Hentschel, B.T., Kaye, S., 2013. Long-term field measurement of sorption of organic contaminants to five types of plastic pellets: implications for plastic marine debris. *Environ. Sci. Technol.* 47 (3), 1646–1654.
- Rotter, G., Ishida, H., 1992. FTIR separation of nylon6 chain conformations: clarification of the mesomorphous and γ crystalline phases. *J. Polym. Sci. B Polym. Phys.* 30 (5), 489–495.
- Ryan, P.G., Moore, C.J., van Franeker, J.A., Moloney, C.L., 2009. Monitoring the abundance of plastic debris in the marine environment. *Philos. Trans. R. Soc. Lond. B Biol. Sci.* 364 (1526), 1999–2012.
- Singh, B., Sharma, N., 2008. Mechanistic implications of plastic degradation. *Polym. Degrad. Stab.* 93 (3), 561–584.
- Tomás, J., Guitart, R., Mateo, R., Raga, J.A., 2002. Marine debris ingestion in loggerhead sea turtles, *Caretta caretta*, from the Western Mediterranean. *Mar. Pollut. Bull.* 44 (3), 211–216.
- Unger, B., Rebolledo, E.L.B., Deaville, R., Gröne, A., IJsseldijk, L.L., Leopold, M.F., Siebert, U., Spitz, J., Wohlsein, P., Herr, H., 2016. Large amounts of marine debris found in sperm whales stranded along the North Sea coast in early 2016. *Mar. Pollut. Bull.* 112 (1), 134–141.
- Verleye, G.A., Roeges, N.P., De Moor, M.O., 2001. *Easy Identification of Plastics and Rubbers*. Rapra Technology Limited, Shropshire, pp. 174.